Magnetic susceptibilities of rare-earth ions in an unusual tetrahedral site

M. R. Roser and L. R. Corruccini

Department of Physics, University of California, Davis, California 95616

(Received 18 August 1989)

Magnetic susceptibilities of the series of compounds $Cs_2NaR(NO_2)_6$ have been measured for most of the rare earths (R) from Ce to Yb. These materials are cubic, with an unusual T_h point symmetry at the rare-earth site. They exhibit not only many similarities but also interesting differences with the related, but octahedrally coordinated, rare-earth elpasolite halides. They are analyzed in terms of a lowest-order crystal-field theory.

I. INTRODUCTION

Crystal-field effects in rare-earth ions located at sites of relatively high symmetry have been studied in only a few solids. This is especially true for insulating compounds, where theoretical analysis is most straightforward, because insulating rare-earth compounds typically crystallize with low symmetry. Early work was confined to systems with symmetry no higher than hexagonal, or utilized rare earths introduced as dopants, without charge compensation, into cubic lattices such as CaF_2 and MgO. The latter technique was useful primarily for magnetic resonance. Cubic materials are especially attractive to study because a theoretical description requires only fourth- and sixth-order crystal-field parameters, and magnetic properties such as Zeeman splittings are often uniquely determined, independent of the size of the crystal-field parameters, for the crystal-field-split states. Since the discovery of the cubic rare-earth elpasolite compounds in 1969, many studies of the magnetic and optical properties of these materials have appeared, particularly the series Cs_2NaRCl_6 (Refs. 1–4) and Rb_2NaRF_6.[5] These compounds are cubic at room temperature, with $Fm3m$ lattice symmetry and octahedral

O_h rare-earth site symmetry. Evidence has accumulated, however, that many of these compounds containing the lighter rare earths undergo a crystalline phase transition below room temperature, and distort typically to tetragonal symmetry.[6–10]

This paper presents a study of the magnetic susceptibility of the related series of compounds $Cs_2NaR(NO_2)_6$. Like the elpasolites, they have a face-centered cubic structure, but with lattice symmetry $Fm3$, and an unusual tetrahedral T_h symmetry at the rare-earth sites. The change in site symmetry leads to some interesting differences in the crystal-field states and the magnetic behavior of the rare-earth ions. In these compounds the rare earths are oxygen coordinated, as occurs also in the rare-earth double nitrates, with sodium ions nitrogen coordinated.[11] A diagram of the crystalline unit cell is shown in Fig. 1. We have synthesized most of the members of this series from Ce to Yb. In contrast to the elpasolite halides, x-ray powder diffraction patterns taken at 10 K indicate that all members of this series maintain their cubic symmetry down to that temperature.

II. EXPERIMENT

Polycrystalline samples of $Cs_2NaR(NO_2)_6$ were obtained as fine precipitates by mixing the appropriate rare-earth chloride or nitrate in water with an excess of $NaNO_2$, and then adding a solution with an excess of CsCl or $CsNO_3$.[12] The excess was sufficient to precipitate virtually all rare-earth ions from solution. Concentrated solutions are required, particularly for the heavier lanthanides. The precipitates were filtered and dried without rinsing, due to their instability in pure water. The individual crystallites are roughly cubic in shape, but show both cubic and octahedral facets. X-ray powder diffraction patterns exhibited face-centered cubic symmetry at all temperatures from 300 to 10 K. All patterns were single phase, with no detectable lines due to $NaNO_2$. CsCl or $CsNO_3$. Unit cell dimensions are listed in Table I. They exhibit the usual lanthanide contraction. Unit cell agreement is good for those compounds that have been measured previously.[11,13,14]

The distance between nearest magnetic ions in this structure is about 7.8 Å and the path between both first
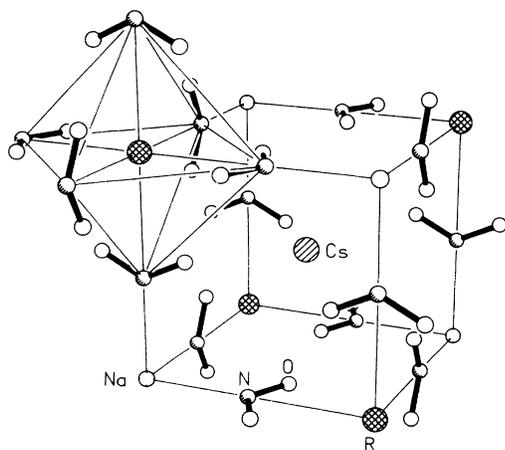
FIG. 1. Diagram of the cubic $Cs_2NaR(NO_2)_6$ lattice. The lattice symmetry is $Fm3$, and the point symmetry at the rare-earth sites is T_h.

TABLE I. Unit cell lengths at 300 K for the series $Cs_2NaR(NO_2)_6$.

	a (Å)	Ferrari et al.[a]	Barnes et al.[b]
$Cs_2NaCe(NO_2)_6$	11.195 98	11.20	11.20
$Cs_2NaPr(NO_2)_6$	11.172 76	11.18	11.15
$Cs_2NaNd(NO_2)_6$	11.154 42		11.321
$Cs_2NaSm(NO_2)_6$	11.110 02		11.10
$Cs_2NaGd(NO_2)_6$	11.084 75		
$Cs_2NaTb(NO_2)_6$	11.078 52		11.06
$Cs_2NaDy(NO_2)_6$	11.061 65		
$Cs_2NaHo(NO_2)_6$	11.057 04		11.05
$Cs_2NaEr(NO_2)_6$	11.043 32		11.05
$Cs_2NaTm(NO_2)_6$	11.036 10		
$Cs_2NaYb(NO_2)_6$	11.019 62		

[a]Reference 13.
[b]References 14 and 11.

and second nearest magnetic neighbors is of the form R-O-N-Na-N-O-R, so the exchange interaction is expected to be small. Susceptibilities measured below 1 K suggest that the primary interaction between ions is magnetic dipolar, with values of the Weiss Θ (dipolar plus exchange) typically smaller than 50 mK in absolute magnitude.

Susceptibility measurements between 2 and 300 K were made with a Quantum Design MPMS SQUID magnetometer, calibrated with a sample of $Gd_2(SO_4)_3 \cdot 8H_2O$ above 20 K. The measuring field was usually 0.05 T. Measurements below 2 K were taken on a number of samples placed in the mixing chamber of a dilution refrigerator, using fluxgate magnetometers.[15] Here the static field was 0.5 mT.

III. THEORY

Group theoretical considerations indicate[16] that a lanthanide ion at a site of T_h symmetry will experience a crystalline electric field with a potential of the form

$$V = B_4^0(O_4^0 + 5O_4^4) + B_6^0(O_6^0 - 21O_6^4) + B_6^2(O_6^2 - O_6^6) ,$$

where the B_n^m are constants and the O_n^m are Stevens operator equivalents.[17] The first two terms describe the potential the ion would experience in a site of cubic (O_h) symmetry; the third is added by the twofold rotational symmetry along the principal cubic axes of the point group T_h. The B_n^m can be further factored into rare-earth ion-specific and ion-independent terms:

$$B_n^m = A_n^m \langle r^n \rangle \theta_n ,$$

where the θ_n and $\langle r^n \rangle$ are different for the various lanthanides, and are tabulated by Elliott and Stevens[18] for the former, and by Freeman and Watson[19] for the latter, in the Hartree-Fock approximation. The A_n^m are in principle ion independent; a point-charge calculation of V due only to the 12 nearest-neighbor oxygen ions yields

$$A_4^0 = -\frac{7Ze^2}{8d^5}(1 - 5\sin^2\theta\cos^2\theta) ,$$

$$A_6^0 = -\frac{3Ze^2}{64d^7}(2 - 21\cos^2\theta\sin^2\theta) ,$$

$$A_6^2 = -\frac{3465Ze^2}{128d^7}(\cos^2\theta - \sin^2\theta)(\cos^2\theta\sin^2\theta) ,$$

where d is the nearest-neighbor distance, Ze is the nearest-neighbor charge, and 2θ is the angle subtended at the rare-earth site by a pair of nearest-neighbor oxygen ions in a NO_2^- radical. This potential reduces to the cubic form in the limits $\theta \to 0$ and $\theta \to \pi/4$, corresponding to octahedral and twelvefold cubic coordination, respectively. Thus one expects that the crystal-field splittings in the rare earths can be derived continuously from those occurring in either an octahedral or a twelvefold cubic site. These have been analyzed by Lea, Leask, and Wolf.[20] For the values of θ expected in these compounds, about 21.7° (almost midway between the two limits), the matrix elements of B_6^2 are smaller than those of B_4^0, but typically larger than those of B_6^0, and it is possible that the "tetrahedral" term $(O_6^2 - O_6^6)$ can be treated as a perturbation. In the analysis that follows, however, we have not used this approach. Matrices for the full crystal-field potential are calculated and diagonalized by computer to predict the order of crystal-field-split states. The sign of A_4^0 is the same as that for octahedral symmetry, but opposite that for twelvefold coordination. In addition, the second nearest neighbors to the rare-earth site (N atoms) are octahedral in coordination, so one might expect the levels in these salts to resemble the octahedral limit more closely than the twelvefold cubic one. This appears to be the case for most of the compounds discussed in the following. The nitrogen distance from the rare-earth site is only about 16% larger than that of the oxygen ions, so they clearly must be included in a point-charge calculation as well. In the following discussion, when point-charge calculations are used for estimates, we will include both types of ions, and assume an approximately equal negative charge for both, as suggested by Kay and Frazer.[21] In reality, of course, the bonding within the NO_2^- radical is at least partially covalent, and the charge distribution is probably not pointlike.

The relation between cubic and T_h crystal-field splittings is as follows. Under cubic symmetry, the $(2J + 1)$-fold degeneracy of a rare earth with integral J is split into singlets A_1 and A_2 (Γ_1 and Γ_2), doublets E (or Γ_3), and two triplets T_1 and T_2 (Γ_4 and Γ_5), which transform as the corresponding irreducible representations of the cubic group O. An ion of half-integral J is split into doublets $\bar{E}_1$ and $\bar{E}_2$ (Γ_6 and Γ_7, or E' and E'') and quartets $\bar{F}$ (Γ_8 or U), which transform as the extra representations of the double cubic group $_{II}O$. Under T_h symmetry the integral J manifold is split into singlets A, E_1, and E_2, ($\Gamma_1, \Gamma_2, \Gamma_3$), the latter two being degenerate Kramers-conjugate states, and triplets T (Γ_4), corresponding to the four irreducible representations of T_h. Half-integral J manifolds split into three types of doublets $\bar{E}$, $\bar{F}_1$, and $\bar{F}_2$, ($\Gamma_5, \Gamma_6, \Gamma_7$), the latter two again degenerate Kramers-

conjugate pairs of states. These transform as the corresponding three extra two-dimensional representations of the double group $_{II}T_h$. When cubic site symmetry is lowered to T_h, the representations A_1 and A_2 reduce to A, E splits into E_1 and E_2, T_1 and T_2 reduce to T, $\bar{E}_1$ and $\bar{E}_2$ reduce to $\bar{E}$, and $\bar{F}$ splits into $\bar{F}_1$ and $\bar{F}_2$. The choice of notation for these states is determined mostly by aesthetics; in the following discussion we employ the spectroscopic notation (A, E_1, etc.) because it displays most clearly the relation between the cubic and tetrahedral eigenfunctions.

The symmetry-adapted angular momentum eigenfunctions of T_h have been derived by Altmann and Cracknell,[22] and by Cracknell and Joshua,[23] in $|L, S\rangle$ notation.

TABLE II. Symmetry-adapted eigenfunctions of J for integral J, corresponding to the irreducible representations of the tetrahedral group T_h, expressed as sums of $|m_J\rangle$ for relevant values of J.

J	State	Wave functions
$J=1$	T	$\|+1\rangle,\ \|-1\rangle,\ \|0\rangle$
$J=2$	E_1	$\dfrac{1}{\sqrt{2}}\|0\rangle-\dfrac{i}{2}(\|+2\rangle+\|-2\rangle)$
	E_2	E_1^*
	T	$\dfrac{1}{\sqrt{2}}(\|2\rangle-\|-2\rangle),\ \|+1\rangle,\ \|-1\rangle$
$J=3$	A	$\dfrac{1}{\sqrt{2}}(\|2\rangle-\|-2\rangle)$
	T	$aT_1+bT_2=a\Gamma_4+b\Gamma_5,\quad$ where $T_1=\{\sqrt{\tfrac{5}{8}}\|\pm3\rangle+\sqrt{\tfrac{3}{8}}\|\mp1\rangle,\|0\rangle\}$
	T	$bT_1-aT_2 \qquad\qquad\qquad T_2=\left\{\sqrt{\tfrac{3}{8}}\|\mp3\rangle-\sqrt{\tfrac{5}{8}}\|\pm1\rangle,\dfrac{1}{\sqrt{2}}(\|2\rangle+\|-2\rangle)\right\}$
$J=4$	A	$\sqrt{\tfrac{5}{24}}\|4\rangle+\sqrt{\tfrac{14}{24}}\|0\rangle+\sqrt{\tfrac{5}{24}}\|-4\rangle$
	E_1	$\sqrt{\tfrac{5}{24}}\|0\rangle-\sqrt{\tfrac{7}{48}}(\|4\rangle+\|-4\rangle)+\dfrac{i}{2}(\|2\rangle+\|-2\rangle)$
	E_2	E_1^*
	T	$aT_1+bT_2,\quad$ where $T_1=\left\{\sqrt{\tfrac{1}{8}}\|\pm3\rangle+\sqrt{\tfrac{7}{8}}\|\mp1\rangle,\dfrac{1}{\sqrt{2}}(\|4\rangle-\|-4\rangle)\right\}$
	T	$bT_1-aT_2 \qquad\qquad T_2=\left\{-\sqrt{\tfrac{7}{8}}\|\mp3\rangle+\sqrt{\tfrac{1}{8}}\|\pm1\rangle,\dfrac{1}{\sqrt{2}}(\|2\rangle-\|-2\rangle)\right\}$
$J=6$	A	$aA_1+bA_2,\quad$ where $A_1=-\sqrt{\tfrac{7}{16}}(\|4\rangle+\|-4\rangle)+\sqrt{\tfrac{1}{8}}\|0\rangle$
	A	$bA_1-aA_2 \qquad\qquad A_2=-\sqrt{\tfrac{5}{32}}(\|6\rangle+\|-6\rangle)+\sqrt{\tfrac{11}{32}}(\|2\rangle+\|-2\rangle)$
	E_1	$\sqrt{\tfrac{7}{16}}\|0\rangle+\sqrt{\tfrac{1}{32}}(\|4\rangle+\|-4\rangle)-i[\sqrt{\tfrac{5}{64}}(\|2\rangle+\|-2\rangle)+\sqrt{\tfrac{11}{64}}(\|6\rangle+\|-6\rangle)]$
	E_2	E_1^*
	$3T$	$a_5\|\pm5\rangle+a_3\|\pm3\rangle+a_1\|\pm1\rangle+a_{-1}\|\mp1\rangle+a_{-3}\|\mp3\rangle+a_{-5}\|\mp5\rangle,$
		$b_6(\|6\rangle-\|-6\rangle)+b_4(\|4\rangle-\|-4\rangle)+b_2(\|2\rangle-\|-2\rangle)$
$J=8$	A	$\sqrt{\tfrac{33}{64}}\|0\rangle+\sqrt{\tfrac{7}{96}}(\|4\rangle+\|-4\rangle)+\sqrt{\tfrac{65}{384}}(\|8\rangle+\|-8\rangle)$
	E_1	$a\|\alpha\rangle+b\|\beta\rangle,\quad$ where $\|\alpha\rangle=\sqrt{\tfrac{31}{128}}\|0\rangle-\sqrt{\tfrac{77}{1984}}(\|4\rangle+\|-4\rangle)-\sqrt{\tfrac{715}{7936}}(\|8\rangle+\|-8\rangle)$
		$\qquad\qquad +i[\sqrt{\tfrac{105}{992}}(\|2\rangle+\|-2\rangle)+\sqrt{\tfrac{143}{992}}(\|6\rangle+\|-6\rangle)]$
	E_1	$b\|\alpha\rangle-a\|\beta\rangle \qquad\qquad \|\beta\rangle=\sqrt{\tfrac{65}{372}}(\|4\rangle+\|-4\rangle)-\sqrt{\tfrac{28}{372}}(\|8\rangle+\|-8\rangle)$
		$\qquad\qquad +i[\sqrt{\tfrac{143}{992}}(\|2\rangle+\|-2\rangle)-\sqrt{\tfrac{105}{992}}(\|6\rangle+\|-6\rangle)]$
	$2E_2$	$2E_1^*$
	$4T$	$a_7\|\pm7\rangle+a_5\|\pm5\rangle+a_3\|\pm3\rangle+a_1\|\pm1\rangle+a_{-1}\|\mp1\rangle+a_{-3}\|\mp3\rangle+a_{-5}\|\mp5\rangle+a_{-7}\|\mp7\rangle,$
		$b_8(\|8\rangle-\|-8\rangle)+b_6(\|6\rangle-\|-6\rangle)+b_4(\|4\rangle-\|-4\rangle)+b_2(\|2\rangle-\|-2\rangle)$

TABLE III. Symmetry-adapted eigenfunctions of J for half-integral J, corresponding to the extra irreducible representations of the double tetrahedral group $_{II}T_h$, expressed as sums of $|m_j\rangle$ for relevant values of J.

J	State	Wave functions
$J=\frac{1}{2}$	$\{\bar{E}$	$\left|\pm\frac{1}{2}\right\rangle$
$J=\frac{3}{2}$	$\bar{F}_1$	$\sqrt{\frac{1}{2}}\left|\pm\frac{1}{2}\right\rangle-\frac{i}{\sqrt{2}}\left|\mp\frac{3}{2}\right\rangle$
	$\bar{F}_2$	$\bar{F}_1^*$
$J=\frac{5}{2}$	$\bar{E}$	$\sqrt{\frac{1}{6}}\left|\pm\frac{5}{2}\right\rangle-\sqrt{\frac{5}{6}}\left|\mp\frac{3}{2}\right\rangle$, $\hat{g}=-\frac{5}{3}$
	$\bar{F}_1$	$\sqrt{\frac{1}{2}}\left|\pm\frac{1}{2}\right\rangle-i\left(\sqrt{\frac{5}{12}}\left|\pm\frac{5}{2}\right\rangle+\sqrt{\frac{1}{12}}\left|\mp\frac{3}{2}\right\rangle\right)$
	$\bar{F}_2$	$\bar{F}_1^*$
$J=\frac{7}{2}$	$\bar{E}$	$a\bar{E}_1+b\bar{E}_2$, where $\left(\bar{E}_1=\sqrt{\frac{7}{12}}\left|\pm\frac{1}{2}\right\rangle+\sqrt{\frac{5}{12}}\left|\mp\frac{7}{2}\right\rangle\right)$, $\hat{g}=-\frac{7}{3}$
	$\bar{E}$	$b\bar{E}_1-a\bar{E}_2$ $\left(\bar{E}_2=\sqrt{\frac{3}{4}}\left|\pm\frac{5}{2}\right\rangle-\frac{1}{2}\left|\mp\frac{3}{2}\right\rangle\right)$, $\hat{g}=3$
	$\bar{F}_1$	$\sqrt{\frac{5}{24}}\left|\pm\frac{1}{2}\right\rangle-\sqrt{\frac{7}{24}}\left|\mp\frac{7}{2}\right\rangle+\frac{i}{2}\left(\sqrt{\frac{1}{2}}\left|\pm\frac{5}{2}\right\rangle+\sqrt{\frac{1}{2}}\left|\mp\frac{3}{2}\right\rangle\right)$
	$\bar{F}_2$	$\bar{F}_1^*$
$J=\frac{9}{2}$	$\bar{E}$	$\sqrt{\frac{7}{12}}\left|\pm\frac{1}{2}\right\rangle+\sqrt{\frac{9}{24}}\left|\pm\frac{9}{2}\right\rangle+\sqrt{\frac{1}{24}}\left|\mp\frac{7}{2}\right\rangle$, $\hat{g}=\frac{11}{3}$
	$\bar{F}_1$	$a|\alpha\rangle+b|\beta\rangle$, where $|\alpha\rangle=\sqrt{\frac{1}{20}}\left|\pm\frac{9}{2}\right\rangle-\sqrt{\frac{9}{20}}\left|\mp\frac{7}{2}\right\rangle+i\left(\sqrt{\frac{3}{20}}\left|\pm\frac{5}{2}\right\rangle-\sqrt{\frac{7}{20}}\left|\mp\frac{3}{2}\right\rangle\right)$
	$\bar{F}_1$	$b|\alpha\rangle-a|\beta\rangle$ $|\beta\rangle=\sqrt{\frac{5}{24}}\left|\pm\frac{1}{2}\right\rangle-\sqrt{\frac{21}{80}}\left|\pm\frac{9}{2}\right\rangle-\sqrt{\frac{7}{240}}\left|\mp\frac{7}{2}\right\rangle+i\left(\sqrt{\frac{7}{20}}\left|\pm\frac{5}{2}\right\rangle+\sqrt{\frac{3}{20}}\left|\mp\frac{3}{2}\right\rangle\right)$
	$2\bar{F}_2$	$2\bar{F}_1^*$

TABLE III. *(Continued).*

J	State	Wave functions
$J = \frac{15}{2}$	$\bar{E}$	$a\bar{E}_1 + b\bar{E}_2$, where $(\bar{E}_1 = \sqrt{\frac{7}{192}}|\pm\frac{9}{2}\rangle + \sqrt{\frac{33}{64}}|\pm\frac{1}{2}\rangle + \sqrt{\frac{7}{64}}|\mp\frac{7}{2}\rangle + \sqrt{\frac{65}{192}}|\mp\frac{15}{2}\rangle$, $\hat{g} = -5)$
	$\bar{E}$	$b\bar{E}_1 - a\bar{E}_2$ $(\bar{E}_2 = \sqrt{\frac{77}{192}}|\pm\frac{13}{2}\rangle + \sqrt{\frac{65}{192}}|\pm\frac{5}{2}\rangle - \sqrt{\frac{39}{192}}|\mp\frac{3}{2}\rangle - \sqrt{\frac{11}{192}}|\mp\frac{11}{2}\rangle$, $\hat{g} = \frac{17}{3})$
	$3\bar{F}_1$	$a|\alpha\rangle + b|\beta\rangle + c|\gamma\rangle$, where $|\alpha\rangle = \sqrt{\frac{3}{8}}|\pm\frac{9}{2}\rangle - \sqrt{\frac{3}{8}}|\pm\frac{1}{2}\rangle - \sqrt{\frac{1}{8}}|\mp\frac{7}{2}\rangle - i(\sqrt{\frac{55}{384}}|\pm\frac{5}{2}\rangle - \sqrt{\frac{91}{384}}|\pm\frac{13}{2}\rangle + \sqrt{\frac{13}{384}}|\mp\frac{11}{2}\rangle)$
		$\quad\quad\quad\quad\quad\quad\quad |\beta\rangle = -\sqrt{\frac{65}{744}}|\pm\frac{9}{2}\rangle - \sqrt{\frac{65}{248}}|\pm\frac{1}{2}\rangle + \sqrt{\frac{14}{93}}|\mp\frac{7}{2}\rangle - i(\sqrt{\frac{429}{3968}}|\pm\frac{5}{2}\rangle + \sqrt{\frac{715}{3968}}|\pm\frac{13}{2}\rangle + \sqrt{\frac{105}{3968}}|\mp\frac{11}{2}\rangle) + \sqrt{\frac{525}{3968}}|\mp\frac{3}{2}\rangle + \sqrt{\frac{735}{3968}}|\mp\frac{11}{2}\rangle)$
		$\quad\quad\quad\quad\quad\quad\quad |\gamma\rangle = -\sqrt{\frac{31}{128}}|\pm\frac{1}{2}\rangle + \sqrt{\frac{77}{3968}}|\mp\frac{9}{2}\rangle + \sqrt{\frac{231}{3968}}|\mp\frac{7}{2}\rangle - i(\sqrt{\frac{315}{3968}}|\pm\frac{5}{2}\rangle + \sqrt{\frac{715}{3968}}|\pm\frac{13}{2}\rangle + \sqrt{\frac{143}{3968}}|\pm\frac{13}{2}\rangle + \sqrt{\frac{1001}{3968}}|\mp\frac{11}{2}\rangle)$
	$3\bar{F}_2^*$	
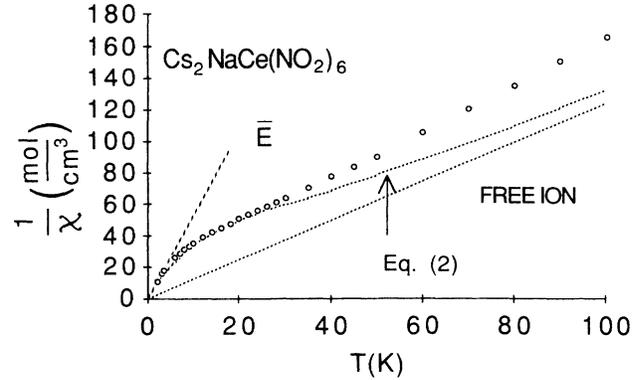
FIG. 2. The inverse of the magnetic susceptibility plotted as a function of temperature for $Cs_2NaCe(NO_2)_6$. The curved line is a fit to Eq. (2); the straight lines correspond to the limiting susceptibilities of the ground state $\bar{E}$ and the free ion.

We list them in Tables II and III in $|J,m\rangle$ notation appropriate for the rare earths. Because the number of irreducible representations of $_{II}T_h$ is smaller than that of $_{II}O$, and their dimensions are smaller (at least on average), there are more repeated representations when the full rotation group is reduced to $_{II}T_h$ than to $_{II}O$. Compared to the cubic case, this results in fewer uniquely specified eigenfunctions, independent of the crystal-field parameters B_n^m, in Tables II and III. For doublets that are unique (and nondegenerate), we also list the reduced spectroscopic splitting factors $\hat{g} = g/g_J = 2\langle n|J_z|n\rangle$, where g_J is the Landé g factor for a particular ion. In general, the g factors are isotropic (except for the degenerate $\bar{F}_1$, $\bar{F}_2$; see the following), and susceptibilities are always so, since the x, y, and z axes are equivalent under T_h. Eigenfunctions corresponding to repeated representations of T_h will depend explicitly on B_4^0, B_6^0, and B_6^2, which are independent quantities. Analysis in this case is thus more complicated than it is for cubic symmetry, where only two independent parameters (B_4^0 and B_6^0) are involved.

IV. RESULTS AND DISCUSSIONS

The susceptibility results that follow are analyzed in terms of the theoretical description of Van Vleck,[24]
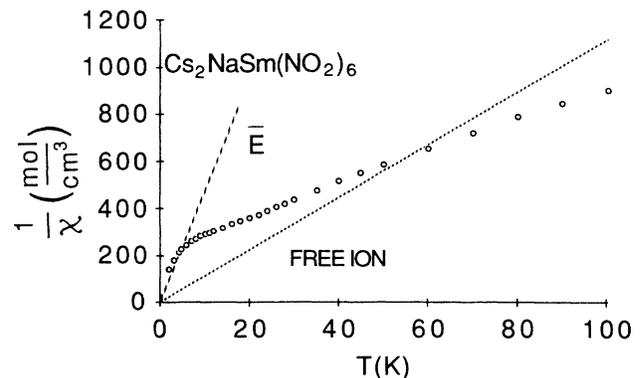
FIG. 3. The inverse susceptibility of $Cs_2NaSm(NO_2)_6$ vs temperature. The straight lines are the calculated ground-state and free-ion susceptibilities.

which includes the effects of crystal-field splittings but neglects interactions between ions. The latter we expect

to be important only well below 1 K. The theoretical expression for susceptibility is

$$\chi = \frac{N_A(g_J\mu_B)^2}{kT} \frac{\sum_n \left[|\langle n|J_z|n\rangle|^2 - 2\sum_{n'} \frac{|\langle n|J_z|n'\rangle|^2 kT}{\mathcal{E}_n - \mathcal{E}_{n'}} \right] e^{-\mathcal{E}_n/kT}}{\sum_n e^{-\mathcal{E}_n/kT}} , \quad (1)$$

where $|n\rangle$ is a crystal-field split state and $\mathcal{E}_n$ is its energy. Because the number of levels which enter this expression can be large $(2J+1)$, with splittings generally unknown, in most cases the analysis will be limited to a determination of the ion's ground state, and in some cases an estimate of the splitting between ground and first excited state.

While the eigenfunctions listed in Tables II and III have the correct transformation properties under T_h, they are not in all cases the correct ones to use for calculating the susceptibility. When the degenerate states $\bar{F}_1, \bar{F}_2$ occur, they cannot be used directly in Eq. (1) because they are not diagonal in J_z. For this reason also they are not the appropriate states to use for calculation of Zeeman splittings, as in a magnetic resonance experiment. Diagonalization of this degenerate subspace leads to eigenfunctions of the form $(\bar{F}_1 + \bar{F}_2)/\sqrt{2}$, $(\bar{F}_1 - \bar{F}_2)/\sqrt{2}$, similar in form to the eigenfunctions of the quartet $\bar{F}$ (Γ_8) under cubic O_h symmetry. The treatment of Zeeman splittings in $\bar{F}_1, \bar{F}_2$ is then parallel to that for the quartet $\bar{F}$.[25] The degenerate E_1, E_2 are similar but nonmagnetic, so this problem does not occur.

Ferromagnetic order has been observed in the Dy, Er, Gd, and Nd salts of this series below 60 mK. These measurements are described in a separate publication.[26]

A. $Cs_2NaCe(NO_2)_6$, $Cs_2NaSm(NO_2)_6$

The Ce^{3+} and Sm^{3+} ions both have a $J = \frac{5}{2}$ ground manifold. Because sixth degree crystal-field terms have no effect on ions with $J = \frac{5}{2}$ or smaller, and because θ_4 (or β) has the same sign for both, we expect a similar order of splittings for the two, and it is interesting to treat them together. The crystal-field Hamiltonian under T_h is identical to that under cubic symmetry in this case. For cubic symmetry, the ground state is predicted by Lea, Leask, and Wolf to be Γ_7 in octahedral symmetry, with a Γ_8 quartet excited state. This is observed in $Cs_2NaCeCl_6$.[1,3] For twelvefold cubic coordination the order of levels is reversed. The only effect of the tetrahedral symmetry is to relabel Γ_7 as $\bar{E}$, and mix Γ_8 into two degenerate doublets $\bar{F}_1$ and $\bar{F}_2$.

Experimental results for $Cs_2NaCe(NO_2)_6$ are shown in Fig. 2 and those for $Cs_2NaSm(NO_2)_6$ in Fig. 3. As in the case of cubic symmetry,[20] a point-charge calculation predicts an $\bar{E}$ (cubic Γ_7) ground state for both, assuming Z is negative, with $\bar{F}_1, \bar{F}_2$ lying 360 B_4^0 above the ground states. These predictions are consistent with the limiting slope of χ^{-1} versus temperature, which is fit closely by

the g factor predicted for $\bar{E}$, $|g|/g_J = \frac{5}{3}$. In the case of Ce^{3+}, a closed-form fit to the expression of Van Vleck is possible:

$$\chi = \frac{N_A(g_J\mu_B)^2}{kT}$$
$$\times \frac{[25 + 160kT/\Delta + e^{-\Delta/kT}(130 - 160kT/\Delta)]}{36(1 + 2e^{-\Delta/kT})} , \quad (2)$$

where Δ is the splitting between $\bar{E}$ and $\bar{F}_1, \bar{F}_2$. This function is identical to the corresponding expression obtained under octahedral symmetry.[3] The fitted Δ is equal to 116 K. Equation (2) is plotted as a solid line in Fig. 2 for this value of Δ, together with the theoretical free-ion susceptibility. In the case of Sm^{3+}, the presence of a low-lying excited manifold with $J = \frac{7}{2}$ at about 1000 cm^{-1} requires a more complicated expression with additional splitting parameters. In Fig. 3 we plot only the limiting susceptibility of $\bar{E}$ and the free-ion expression for $J = \frac{5}{2}$.

B. $Cs_2NaPr(NO_2)_6$

This material has perhaps the most unusual susceptibility of any compound in the series, as shown in Fig. 4. Two different samples exhibited identical susceptibilities. In an octahedral site Pr^{3+} has a singlet A_1 (Γ_1) ground state for any ratio of fourth to sixth-order crystal-field parameters.[20] This produces a temperature-independent Van Vleck susceptibility at low temperatures, as observed in the Pr elpasolite halides.[1,3,5] In the twelvefold coordinated cubic case, the ground state is expected to be either $T_2(\Gamma_5)$ or $E(\Gamma_3)$. $Cs_2NaPr(NO_2)_6$, in contrast to the octahedral case, exhibits a susceptibility which increases monotonically down to the lowest temperatures obtained, about 6 mK. Furthermore, the limiting slope of χ^{-1} as a function of T changes substantially below about 0.25 K, suggesting a very small splitting between ground and first excited states. The limiting slope below 15 mK yields a very small moment, with a Curie constant of 0.041 cm^3 K/mol. In a site of T_h symmetry, the $J = 4$ manifold of Pr^{3+} is split into a singlet A, degenerate singlets E_1, E_2, and two triplets T. In this case it is possible to obtain explicit expressions for the energies $\mathcal{E}$ of these states in terms of the crystal-field parameters:

$$\mathcal{E}_A = 28b_4 - 80b_6 ,$$

$$\mathcal{E}_{E_1,E_2} = 4b_4 + 64b_6 ,$$

$$\mathcal{E}_{T^{(1)},T^{(2)}} = -6b_4 - 8b_6 \pm [(20b_4 + 12b_6)^2 + (t_6)^2]^{1/2} ,$$
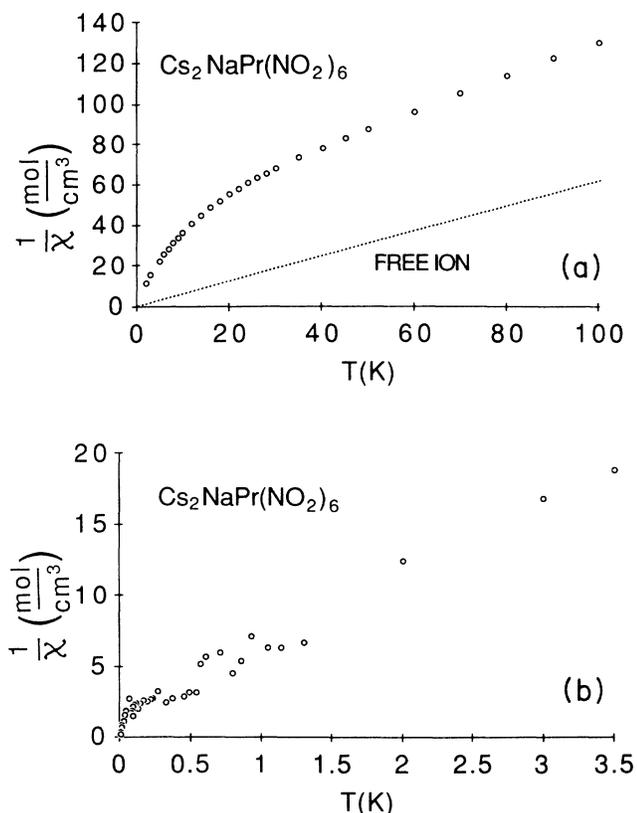
FIG. 4. Inverse susceptibility vs T of $Cs_2NaPr(NO_2)_6$. The behavior below 4 K is expanded.

where $b_4 = 60B_4^0$, $b_6 = 1260B_6^0$, and $t_6 = 1440\sqrt{7}B_6^2$. The tetrahedral term t_6 enters into the triplet energies only; the singlet levels are unchanged from their expressions in the cubic case. In the likely case of b_4 negative, with $|b_4| \gg |b_6|$, A will again be the ground state, as for octahedral symmetry, with $T^{(1)}$ the first excited state, unless t_6 is rather large in magnitude in which case the two will be inverted. A point-charge calculation yields $t_6 \simeq 5b_4$, so the latter is not out of the question, particularly if B_6^0 is negative (opposite to the octahedral case).[20] The experimental low-temperature g factor, $|g| = 0.405$ (effective spin 1) is also very close in magnitude to that of the cubic T_1 ($g=0.4$), and within the range of possible values for a triplet ground state ($0.4 < g < 2$).

Another possibility is a singlet ground state, split by a very small energy from an excited triplet. Because the matrix elements of J_z between either triplet and both A and E_1, E_2 are nonzero, one might suppose that a sufficiently small splitting could account for the observed behavior. This appears doubtful; even if the splitting were sufficiently small (less than 100 mK), the calculated matrix elements lead to low-temperature Curie constants, which are many times larger than observed. We conclude that the most likely ground state is a triplet derived largely from T_1.

C. $Cs_2NaNd(NO_2)_6$

A cubic crystal-field splits the $^4I_{9/2}$ ground manifold of Nd^{3+} into a doublet $\bar{E}_1$ (Γ_6) and two quartets $\bar{F}$ ($\Gamma_8^{(1)}$ and
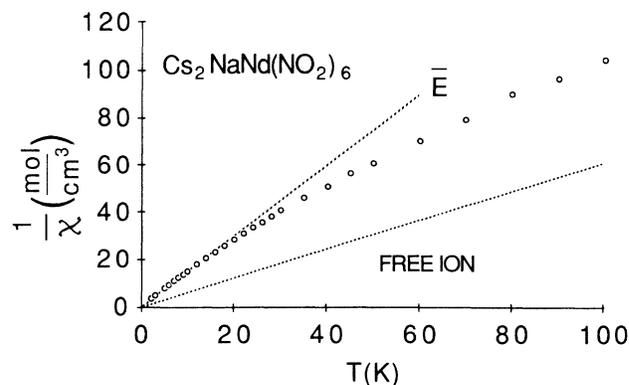
FIG. 5. Measured and calculated inverse susceptibilities of $Cs_2NaNd(NO_2)_6$.

$\Gamma_8^{(2)}$). The ground state is expected to be either $\bar{E}_1$ or $\bar{F}^{(2)}$ in an octahedral environment, depending on the ratio of B_4^0 to B_6^0, and either $\bar{E}_1$ or $\bar{F}^{(1)}$ for a twelvefold cubic environment. In the related Nd elpasolite chloride the ground state is observed to be $\bar{F}$.[1,3] In the T_h symmetry of $Cs_2NaNd(NO_2)_6$, $\bar{E}_1$ becomes $\bar{E}$ but is unchanged in functional form, while the two quartets both mix into degenerate pairs of Kramers-conjugate doublets. In contrast to the elpasolite case, the limiting low-temperature susceptibility yields a g factor nearly identical to that predicted for $\bar{E}$, $g = \frac{8}{3}$, as shown in Fig. 5. Under the assumption that the charges on the nearest-neighbor oxygen ions are negative, a point-charge calculation also predicts $\bar{E}$ to be the ground state.

D. $Cs_2NaGd(NO_2)_6$

In common with most gadolinium salts, this material exhibits a rather featureless susceptibility down to temperatures comparable to the residual magnetic dipole interaction energy, about 0.1 K (Fig. 6). From the Curie constant above ~ 10 K we infer a g factor of 1.89, in approximate agreement with the free-ion prediction of 2.00.

E. $Cs_2NaTb(NO_2)_6$ and $Cs_2NaTm(NO_2)_6$

There is a close parallel between these compounds and the analogous Tb and Tm elpasolite halides. In a cubic field the $J=6$ ground manifold of Tb^{3+} and Tm^{3+} splits
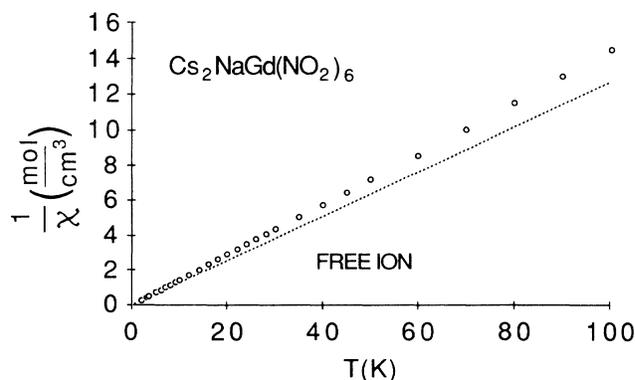
FIG. 6. Measured inverse susceptibility of $CsNaGd(NO_2)_6$.
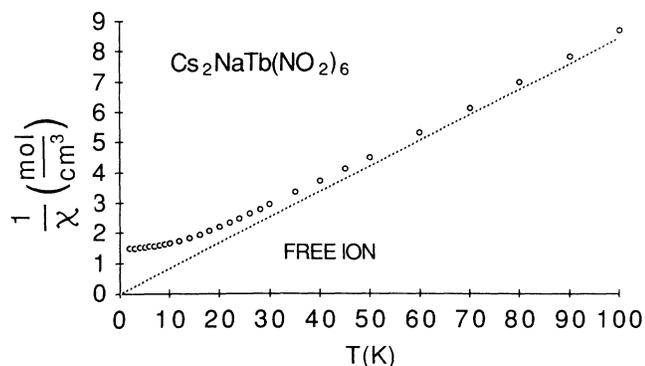
FIG. 7. Measured inverse susceptibility of $Cs_2NaTb(NO_2)_6$.

into singlets A_1 and A_2, a doublet E, a triplet T_1, and two triplets T_2. For octahedral coordination one expects a ground state of A_1 or A_2; for twelve-fold coordination, E or $T_2^{(1)}$. Under T_h these states become two singlets A, two Kramers-conjugate singlets E_1,E_2, and three triplets, T. We find the susceptibilities and the inferred splitting patterns in these compounds to be similar, so they will be discussed together. In the case of the octahedral elpasolite halides,[1,3,5] both Tb^{3+} and Tm^{3+} exhibit temperature-independent paramagnetism at low temperature, and the best-fit ground state is inferred to be A_1. We observe similar susceptibilities in $Cs_2NaTb(NO_2)_6$ and $Cs_2NaTm(NO_2)_6$, as shown in Figs. 7 and 8. A point-charge estimate puts a singlet A as the ground state in both cases, with next excited state $T^{(1)}$, followed by $T^{(2)}$, $A^{(2)}$, $T^{(3)}$, and E_1,E_2. The matrix elements of the tetrahedral term $B_6^2(O_6^2-O_6^6)$ are rather small here, and the sequence of states is identical to that expected in octahedral symmetry. The form of the wave functions is different, however, and the limiting low-temperature induced susceptibility, from (1), is due to matrix elements between the ground state $A^{(1)}$ and all three triplets T. For this reason it is not possible to obtain any level splittings from $\chi(T=0)$.

F. $Cs_2NaDy(NO_2)_6$

The $^6H_{15/2}$ ground manifold of D_y^{3+} is split by a cubic field into doublets $\bar{E}_1$ and $\bar{E}_2$, and three quartets $\bar{F}$. Oc-

tahedral Dy^{3+} has possible ground states of $\bar{E}_1$ and $\bar{E}_2$.[20] This is observed in $Cs_2NaDyCl_6$ which has a reported ground state of $\bar{E}_1$ (Γ_6), with a theoretical g factor of 6.67.[3] In twelvefold cubic coordination, the predicted ground state is $\bar{F}$ (Γ_8). When the site symmetry is changed to T_h, $\bar{E}_1$ and $\bar{E}_2$ mix to form two doublets $\bar{E}$, and the three quartets mix to form three pairs of degenerate Kramers-conjugate doublets $\bar{F}_1,\bar{F}_2$. A point-charge calculation puts $\bar{E}$ lowest, as for octahedral symmetry. The two doublets $\bar{E}$ are of the form $a\bar{E}_1+b\bar{E}_2$, $b\bar{E}_1-a\bar{E}_2$, with energies

$$\mathscr{E}=\tfrac{1}{2}\{\mathscr{E}_1+\mathscr{E}_2\pm[(\mathscr{E}_1-\mathscr{E}_2)^2+(t_6)^2]^{1/2}\}\ ,$$

where

$$\mathscr{E}_1=294b_4-40b_6,\quad b_4=60B_4^0\ ,$$

$$\mathscr{E}_2=-26b_4-312b_6,\quad b_6=13\,860B_6^0\ ,$$

$$t_6=147\,840(\tfrac{39}{77})^{1/2}B_6^2\ ,$$

and where $\mathscr{E}_1$ is the energy of $\bar{E}_1$ and $\mathscr{E}_2$ the energy of $\bar{E}_2$ in cubic symmetry. For Dy^{3+} in octahedral symmetry, b_4 is negative and expected to be larger in magnitude than b_6. The addition of the tetrahedral term t_6 does not change the relative order of the doublets $\bar{E}_1$ and $\bar{E}_2$, but increases the magnitude of the energy of $\bar{E}_1$, i.e., it drives it lower. If B_6^0 is positive, similar to the octahedral case, the probable ground state of Dy^{3+} in $CsNaDy(NO_2)_6$ remains $\bar{E}$, and is largely derived from the octahedral $\bar{E}_1$. If B_6^0 is negative, $\bar{F}_1,\bar{F}_2$ is also a possible ground state.[20]

The experimental susceptibility of $Cs_2NaDy(NO_2)_6$ is shown in Fig. 9. It shows noticeable curvature below 0.5

(a)

FIG. 8. Measured inverse susceptibility of $Cs_2NaTm(NO_2)_6$.

(b)
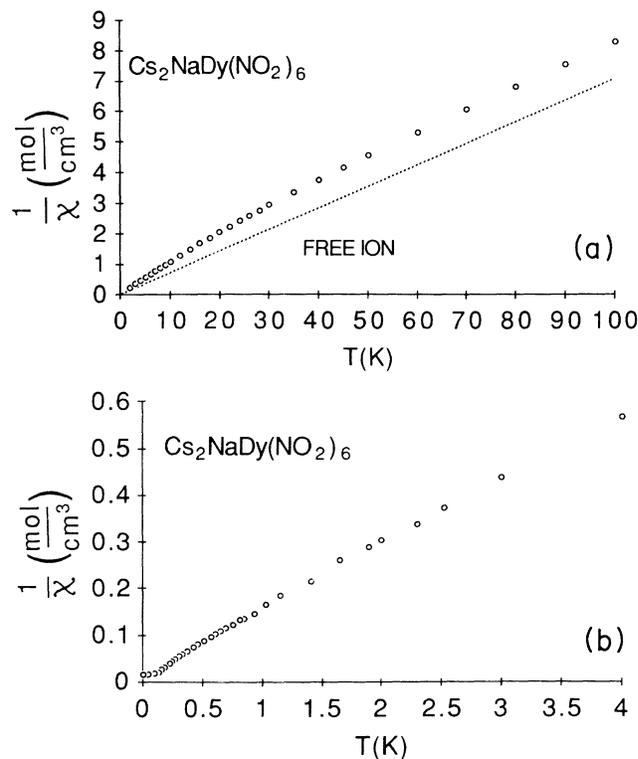
FIG. 9. Measured inverse susceptibility of $Cs_2NaDy(NO_2)_6$.

K, suggesting a very small splitting between ground and first excited states. It is difficult to obtain an accurate ground-state Curie constant from this data, since the effect of interactions between ions becomes appreciable below this temperature. Data between 0.2 and 0.4 K yield an approximate Curie constant of 5.01 cm^3 K/mol, implying a doublet g factor of magnitude 7.3. While this is barely consistent with an $\bar{E}$ ground state $(-6.67 < g < 7.56)$, it is not consistent with one consisting mostly of $\bar{E}_1$. Data above 0.5 K yields a larger Curie constant consistent only with $\bar{F}_1, \bar{F}_2$. A preliminary EPR spectrum of a polycrystalline sample of Dy^{3+} doped $Cs_2NaY(NO_2)_6$ exhibits two broad peaks, also consistent with $\bar{F}_1, \bar{F}_2$. We conclude that, on balance, the data favors a ground state of $\bar{F}_1, \bar{F}_2$, implying $B_6^0 < 0$. A more accurate determination of the ground state of this salt must await single-crystal EPR measurements, upon which we are now working.

G. Cs$_2$NaHo(NO$_2$)$_6$

The susceptibility of this compound shows temperature-independent paramagnetism below ~10 K, as shown in Fig. 10. This is similar to the behavior of Ho^{3+} in the elpasolite halides, [1,3,5] where the ground state is found to be $\bar{E}^{(2)}$ ($\Gamma_3^{(2)}$). For twelve-fold cubic coordination, the expected ground state is T_2, which our observations probably rule out. Excited states in the octahedral case are $T_1^{(2)}$, A_1, $T_1^{(1)}$, $T_2^{(2)}$, $\bar{E}^{(1)}$, and $T_2^{(1)}$. The splitting between the lowest three states is small, and the three levels cross for a particular ratio of B_4^0 to B_6^0. A point-charge calculation for $Cs_2NaHo(NO_2)$ exhibits similar behavior; either A or E_1, E_2 are possible ground states, depending on B_4^0/B_6^0, with T with first excited state, and splittings between the three rather small. As in the elpasolite case, either ground state has off-diagonal elements of J_z with all the triplets, so no splittings can be obtained from $\chi(T=0)$.

H. Cs$_2$NaEr(NO$_2$)$_6$

This material also appears to resemble the corresponding elpasolite chloride. In that case, an octahedral crystal-field splits the $J = \frac{15}{2}$ ground manifold of Er^{3+} into doublets $\bar{E}_1$ and $\bar{E}_2$ (Γ_6 and Γ_7) and three quartets $\bar{F}$ (Γ_8), just as for Dy^{3+}. The ground state is predicted[20] to

FIG. 11. Measured inverse susceptibility of Cs$_2$NaEr(NO$_2$)$_6$.

be $\bar{E}_2$ or $\bar{F}$ (Γ_7 or Γ_8) for octahedral, and $\bar{E}_1$ or $\bar{F}$ for twelvefold, symmetries; experimentally $\bar{F}$ is found in Er^{3+} doped Cs_2NaYCl_6.[27] The susceptibility data for $Cs_2NaEr(NO_2)_6$, shown in Fig. 11, are consistent only with the analogous ground state under T_h symmetry, $\bar{F}_1, \bar{F}_2$. If the ground state is assumed to be a (nondegenerate) doublet, the low-temperature limiting Curie constant yields $g = 8.0$, outside the possible limits for $\bar{E}$ $(-6 < g_{\bar{E}} < 6.8)$.

I. Cs$_2$NaYb(NO$_2$)$_6$

Departures from cubic behavior are particularly visible in this salt. In cubic symmetry the $J = \frac{7}{2}$ ground manifold of Yb^{3+} splits into the nonrepeated states $\bar{E}_1$, $\bar{E}_2$, and $\bar{F}$. Thus the low-temperature susceptibility of Yb^{3+} in a cubic environment must display one of three unique Curie constants: $C_{\bar{E}_1} = 0.667$ cm^3 K/mol $(g = -\frac{8}{3})$, $C_{\bar{E}_2} = 1.1025$ cm^3 K/mol $(g = \frac{24}{7})$, and $C_{\bar{F}} = 0.88473$ cm^3 K/mol. Experimentally $Cs_2NaYbCl_6$ is found to have an $\bar{E}_1$ ground state.[2,3] $Cs_2NaYb(NO_2)_6$, by contrast, has a low-temperature Curie constant which is considerably smaller than any of these values at $C = 0.146$ cm^3 K/mol (Fig. 12). This is consistent only with a ground state $\bar{E}$, which is a mixture of the cubic $\bar{E}_1$ and $\bar{E}_2$, and has a g factor bounded by their values.

This ground state is also predicted by a diagonalization

FIG. 10. Measured inverse susceptibility of Cs$_2$NaHo(NO$_2$)$_6$.
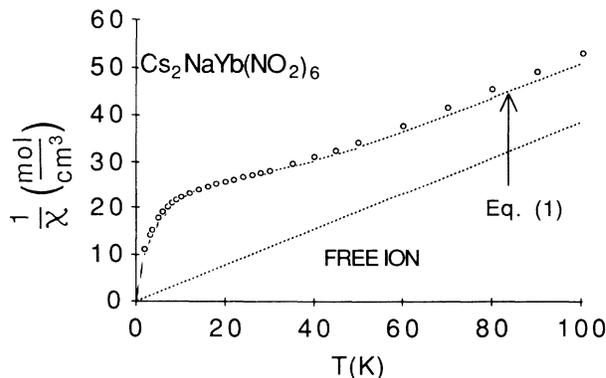
FIG. 12. Measured and calculated inverse susceptibilities of Cs$_2$NaYb(NO$_2$)$_6$.

of the crystal-field Hamiltonian, which yields

$$\mathcal{E}_{\bar{E}} = \tfrac{1}{2}\{\mathcal{E}_1 + \mathcal{E}_2 \pm [(\mathcal{E}_1 - \mathcal{E}_2)^2 + (t_6)^2]^{1/2}\} \ ,$$

$$\mathcal{E}_{\bar{F}_1,\bar{F}_2} = 2b_4 + 16b_6 \ ,$$

where $\mathcal{E}_1$ and $\mathcal{E}_2$ correspond to the energies of $\bar{E}_1$ and $\bar{E}_2$ and are equal to $14b_4 - 20b_6$ and $-18b_4 - 12b_6$, respectively. Here $b_4 = 60B_4^0$, $b_6 = 1260B_6^0$, and $t_6 = 576\sqrt{35}B_6^2$. If one adopts the point-charge prediction of B_4^0 negative, with $|B_4^0| \gg |B_6^0|$, this predicts that the doublet evolving from the octahedral E_1 will be driven lower in energy by the tetrahedral term t_6, and one expects it to remain the ground state.

The low-temperature Curie constant yields mixing factors of $a = 0.876$ or 0.598. If we assume the ground state is composed mostly of $\bar{E}_1$, the former is the correct value. Using this mixing ratio a fit to Eq. (1) is also shown in Fig. 12. The first excited state is $\bar{F}_1, \bar{F}_2$, with $\bar{E}^{(2)}$ highest, as in the octahedral case.[3] The best-fit splitting values are $\Delta_{\bar{F}_1,\bar{F}_2 - \bar{E}^{(1)}} = 123$ K, $\Delta_{\bar{E}^{(2)} - \bar{E}^{(1)}} = 650$ K. These splittings are not very sensitive to the choice of mixing ratio. The latter splitting can be expressed in terms of B_6^2 and the mixing ratio a/b alone:

$$\Delta_{\bar{E}^{(2)} - \bar{E}^{(1)}} = 288\sqrt{35}B_6^2 \left| \frac{a}{b} + \frac{b}{a} \right| \ .$$

From this we obtain $|B_6^2| = 0.16$ K.

V. SUMMARY AND CONCLUSIONS

Rare-earth ions in the tetrahedral sites of $Cs_2NaR(NO_2)_6$ exhibit magnetic susceptibilities which show close parallels, but also interesting differences, with the octahedrally coordinated compounds Cs_2NaRCl_6 and Rb_2NaRF_6. Exceptions to this correspondence are exhibited by Pr^{3+} and possibly Dy^{3+}, where further work is needed to definitely establish the ground state. In general, where crystal-field splittings can be estimated, they appear to be smaller than in the Cs_2NaRCl_6. This may be due to the slightly larger lattice constants in the nitrites, or possibly because the charge distribution of the NO_2^- radical is spread out more than that of Cl^-. The susceptibilities appear to be generally consistent with the assumption that $|B_4^0| \gg |B_6^0|$, as found in other cubic rare-earth materials.[25] In most of the $Cs_2NaR(NO_2)_6$, the analysis is not very sensitive to the sign assumed for B_6^0. In a few (Pr,Nd,Dy), there is some evidence that B_6^0 may have the sign opposite to that which occurs in octahedral symmetry.

ACKNOWLEDGMENTS

[1]M. V. Hoehn and D. G. Karraker, J. Chem. Phys. **60**, 393 (1974).

[2]D. G. Karraker, J. Chem. Phys. **55**, 1084 (1971).

[3]B. D. Dunlap and G. K. Shenoy, Phys. Rev. B **12**, 2716 (1975).

[4]D. R. Foster and F. S. Richardson, J. Chem. Phys. **82**, 1085 (1985), and references therein.

[5]E. Bucher, H. J. Guggenheim, K. Andres, G. W. Hull, Jr., and A. S. Cooper, Phys. Rev. B **10**, 2945 (1974).

[6]B. Bleaney, A. G. Stephen, P. J. Walker, and M. R. Wells, Proc. R. Soc. London, Ser. A **381**, 1 (1982); ibid. **376**, 235 (1981).

[7]G. P. Knudsen, F. W. Voss, and R. Nevald, in *The Rare Earths in Modern Science and Technology*, edited by G. J. McCarthy, H. B. Silber, and J. J. Rhyne (Plenum, New York, 1982), Vol. 3, p. 335.

[8]R. W. Schwartz, Mol. Phys. **30**, 81 (1975).

[9]E. J. Veenendal, H. B. Brom, and J. Ihringer, Physica **114B**, 31 (1982).

[10]G. Meyer, Prog. Solid State Chem. **14**, 141 (1982).

[11]J. C. Barnes, K. Al-Rasoul, and P. Harkins, J. Chem. Soc. Pak. **2**, 9 (1980).

[12]H. C. Goswami and P. B. Sarkar, J. Indian Chem. Soc. **12**, 608 (1935).

[13]A. Ferrari, L. Cavalca, and M. Nardelli, Gazz. Chim. Ital. **81**, 1082 (1951).

[14]J. C. Barnes and R. D. Peacock, J. Chem. Soc. A **558** (1971).

[15]K. Andres and J. H. Wernick, Rev. Sci. Instrum. **44**, 1186 (1973).

[16]J. L. Prather, *Atomic Levels in Crystals*, Natl. Bur. Stand. (U.S.) Monograph No. 19 (U.S. GPO, Washington, D.C., 1961), p. 14.

[17]M. T. Hutchings, *Solid State Physics*, edited by F. Seitz and D. Turnbull (Academic, New York, 1964), Vol. 16, p. 227.

[18]R. J. Elliott and K. W. H. Stevens, Proc. R. Soc. London, Ser. A **218**, 553 (1953).

[19]A. J. Freeman and R. E. Watson, Phys. Rev. **127**, 2058 (1962).

[20]K. R. Lea, M. J. M. Leask, and W. P. Wolf, J. Phys. Chem. Solids **23**, 1381 (1962).

[21]M. I. Kay and B. C. Frazer, Acta Crystallogr. **14**, 56 (1961).

[22]S. L. Altmann and A. P. Cracknell, Rev. Mod. Phys. **37**, 19 (1965).

[23]A. P. Cracknell and S. J. Joshua, Proc. Cambridge Philos. Soc. **67**, 647 (1970); see also C. J. Bradley and A. P. Cracknell, *The Mathematical Theory of Symmetry in Solids* (Clarendon, Oxford, 1972).

[24]J. H. Van Vleck, *Theory of Electric and Magnetic Susceptibilities* (Clarendon, Oxford, 1932).

[25]A. Abragam and B. Bleaney, *Electron Paramagnetic Resonance of Transition Ions* (Clarendon, Oxford, 1970), Sec. 18.3

[26]M. R. Roser and L. R. Corruccini (unpublished).

[27]C. J. O'Connor, R. L. Carlin, and R. W. Schwartz, J. Chem. Soc. Farad. Trans. II **73**, 361 (1977).